Correlations after Quantum Quenches in the *XXZ* Spin Chain: Failure of the Generalized Gibbs Ensemble

B. Pozsgay,[1] M. Mestyán,[1] M. A. Werner,[2] M. Kormos,[1] G. Zaránd,[2] and G. Takács[1,*]

[1]*MTA-BME "Momentum" Statistical Field Theory Research Group, Department of Theoretical Physics,*
Budapest University of Technology and Economics, 1111 Budapest, Budafoki út 8, Hungary
[2]*MTA-BME "Momentum" Exotic Quantum Phases Research Group, Department of Theoretical Physics,*
Budapest University of Technology and Economics, 1111 Budapest, Budafoki út 8, Hungary

We study the nonequilibrium time evolution of the spin-1/2 anisotropic Heisenberg (*XXZ*) spin chain, with a choice of dimer product and Néel states as initial states. We investigate numerically various short-ranged spin correlators in the long-time limit and find that they deviate significantly from predictions based on the generalized Gibbs ensemble (GGE) hypotheses. By computing the asymptotic spin correlators within the recently proposed quench-action formalism [Phys. Rev. Lett. **110**, 257203 (2013)], however, we find excellent agreement with the numerical data. We, therefore, conclude that the GGE cannot give a complete description even of local observables, while the quench-action formalism correctly captures the steady state in this case.

PACS numbers: 75.10.Jm, 02.30.Ik, 05.70.Ln

Introduction.—Recent, spectacular advances in the field of ultracold atoms enabled experimentalists to investigate the coherent time evolution of almost perfectly isolated quantum many-body systems [1–4]. These new developments triggered tremendous theoretical interest [5–18] in a long-standing problem of fundamental physical importance: do isolated quantum systems reach an equilibrium in some sense, and if the answer is positive, what is the nature of the steady state reached?

In the absence of external driving forces, generic systems are expected to reach a steady state locally indistinguishable from thermal equilibrium [5,7]. However, integrable systems behave differently because conservation of the expectation values of extra local charges prevents relaxation to a thermal state. It was suggested in Ref. [19] that in the integrable case the long-time asymptotic stationary state is described by a statistical ensemble involving all the local conserved charges $\{\hat{Q}_i\}$, the generalized Gibbs ensemble (GGE), defined by the density matrix

$$\hat{\rho}_{\text{GGE}} = \frac{1}{Z} e^{-\sum_i \beta_i \hat{Q}_i}, \qquad Z = \text{Tr} e^{-\sum_i \beta_i \hat{Q}_i}, \qquad (1)$$

where the "chemical potentials" $\{\beta_i\}$ are determined by the expectation values of the charges in the ensemble and the initial quantum state.

The GGE idea has by now become widely accepted in the field and has been verified in several specific cases. Until recently, however, most investigations concerning GGE were carried out in theories equivalent to free fermions [20–29] or by numerical studies of relatively small systems [30,31]. It is only recently that it has become possible to examine genuinely interacting integrable systems such as the one-dimensional Bose gas [32–34], the *XXZ* Heisenberg spin chain [35–37], or field theories [38–40].

However, until now there have only been a few precision numerical tests for the predictions of the GGE against real-time dynamics [37]. In our Letter, we perform real-time numerical simulations on a genuinely interacting quantum system, the anisotropic Heisenberg model, and compare the relaxation of various local spin-spin correlation functions to the predictions of two competing theories: the overlap-incorporating thermodynamic Bethe ansatz (OTBA) approach, which implements the quench-action method [41], and the widely accepted GGE.

In agreement with some recent observations [42,43], we find that these two approaches yield markedly different predictions. We arrive at a surprising conclusion: while the numerical results agree spectacularly with the OTBA, they differ significantly from the exact predictions of the GGE in a number of cases (see Fig. 2). These results lead to the inevitable conclusion that the GGE approach fails as a generic description of steady states in genuinely interacting integrable quantum systems.

Quantum quench in the XXZ chain.—The *XXZ* Heisenberg chain is a chain of $s = 1/2$ spins interacting via the Hamiltonian

$$H = -\sum_{i=1}^{L} [\sigma_i^x \sigma_{i+1}^x + \sigma_i^y \sigma_{i+1}^y + \Delta(\sigma_i^z \sigma_{i+1}^z - 1)], \qquad (2)$$

where $\sigma_i^{x,y,z}$ are the Pauli matrices at site i. This model describes magnetism in real compounds [44] and plays a fundamental role in the theory of strongly correlated condensed-matter systems [45]. Here, we focus on the Ising regime $\Delta > 1$, which corresponds to a gapped antiferromagnetic phase in equilibrium.

We implement the nonequilibrium process via the paradigmatic setting of quantum quench [46,47], whereby

the time evolution of the system starts from the ground state of some Hamiltonian but then at time $t = 0$ some parameter of the system is abruptly changed. Quantum quenches of this kind can be implemented in a controlled fashion by realizing the *XXZ* chain in systems of cold atoms in optical lattices [48–52].

As initial states, we consider the translationally invariant projection of the Néel state

$$|\Psi_0^N\rangle = \frac{1 + \hat{T}}{\sqrt{2}}|\uparrow\downarrow\uparrow\ldots\rangle = \frac{1}{\sqrt{2}}(|\uparrow\downarrow\uparrow\ldots\rangle + |\downarrow\uparrow\downarrow\ldots\rangle), \quad (3)$$

which is a ground state in the $\Delta \to \infty$ limit, and the similarly symmetrized dimer product state

$$|\Psi_0^D\rangle = \frac{1 + \hat{T}}{\sqrt{2}}\left|\frac{(\uparrow\downarrow - \downarrow\uparrow)}{\sqrt{2}}\frac{(\uparrow\downarrow - \downarrow\uparrow)}{\sqrt{2}}\ldots\right\rangle, \quad (4)$$

which is one of the ground states of the Majumdar-Ghosh Hamiltonian [53]. Here, $\hat{T}$ is the one site translation operator on the lattice. It is expected that ground states of local Hamiltonians always relax to a steady state.

Failure of the GGE description of the steady-state correlations.—To demonstrate that the GGE cannot give an appropriate description of the steady state, we compare its predictions for correlation functions with the results of real-time out-of-equilibrium numerical simulations, performed using the infinite size time evolving block decimation (ITEBD) algorithm [54,55]. In the simulations, translational invariance of the initial states in Eqs. (3) and (4) was implemented by averaging over the two components of the states [56]. The time evolution of three different correlators is shown in Fig. 1 for a quench starting from the dimer state for $\Delta = 4$ (red lines). The correlation functions quickly converge to stationary values before the simulations break down for large times (shaded regions) [57].

Strikingly, the exact GGE values of Ref. [37] (blue dotted lines in Fig. 1) deviate significantly from the ITEBD results. We report similar deviations for all $\Delta > 1$ in Fig. 2, where we display the long-time asymptotic values extracted from

the ITEBD simulation (red circles) together with the GGE predictions (squares) for $\langle\sigma_1^z\sigma_2^z\rangle$ and $\langle\sigma_1^z\sigma_3^z\rangle$, as functions of Δ. We included truncated GGE (TGGE) results [35,36] as well, obtained by keeping the first six nonzero charges in the density matrix (1). The discrepancy between the GGE and the ITEBD results is evident (for additional numerical data, see the Supplemental Material [58]).

The mismatch between real-time simulations and GGE results could be, in principle, the result of long relaxation times beyond the reach of the ITEBD simulations. We rule out this possibility by applying an alternative theoretical method, the overlap thermodynamic Bethe ansatz (OTBA) which implements the quench-action method [34,41] (see below), and predicts *exactly* the asymptotic values of the correlations. These values, shown as black dashed lines in Fig. 1 and black stars in Fig. 2, are clearly in excellent agreement with our ITEBD results. The state predicted by the OTBA is a steady state of maximal conditional entropy. Therefore, the excellent agreement proves that the ITEBD simulation has reached the true asymptotic steady state and, thus, makes the evidence for the breakdown of the GGE conclusive. Moreover, it also demonstrates that the quench-action-approach-based OTBA indeed correctly captures the steady state of the *XXZ* model.

The TGGE predictions evaluated in Ref. [35] and the OTBA results are also different in the Néel case, but for large Δ, where the TGGE is reliable, this difference is beyond our numerical resolution (Supplemental Material [58]). We obtained similar results for *x*-*x* correlators for both initial states, although for the latter ITEBD is not as accurate as for the *z*-*z* correlators (cf. Ref. [59]).

We remark that translational invariance would be broken for the dimer state without the symmetrization under $\hat{T}$ in Eqs. (3) and (4), and it is yet an open question whether it is restored in the long-time limit after the quench [27,37]. Nevertheless, the GGE was expected to describe the average over the two components of the states of Eqs. (3) and (4), and yet it fails to do so. Note that for the observable $\langle\sigma_1^z\sigma_3^z\rangle$ translational averaging is immaterial since it is identical on both sublattices.
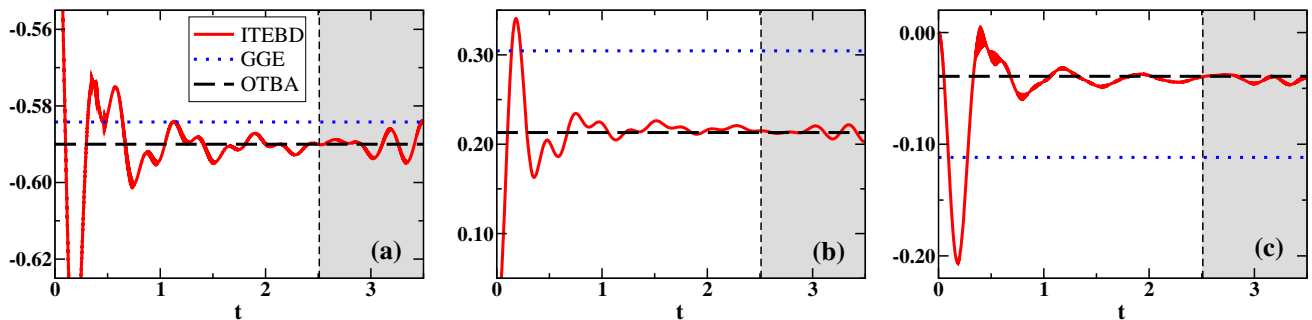

FIG. 1 (color online).   Numerical simulation of the time evolution of correlation functions (a) $\langle\sigma_1^z\sigma_2^z\rangle$, (b) $\langle\sigma_1^z\sigma_3^z\rangle$, (c) $\langle\sigma_1^z\sigma_4^z\rangle$ starting from the dimer initial state (4) for anisotropy $\Delta = 4$ as obtained by ITEBD (red lines). In the shaded region, the results are not reliable. The horizontal lines show the GGE prediction [37] (blue dotted lines) and the prediction of the overlap TBA of the quench-action approach (black dashed lines).
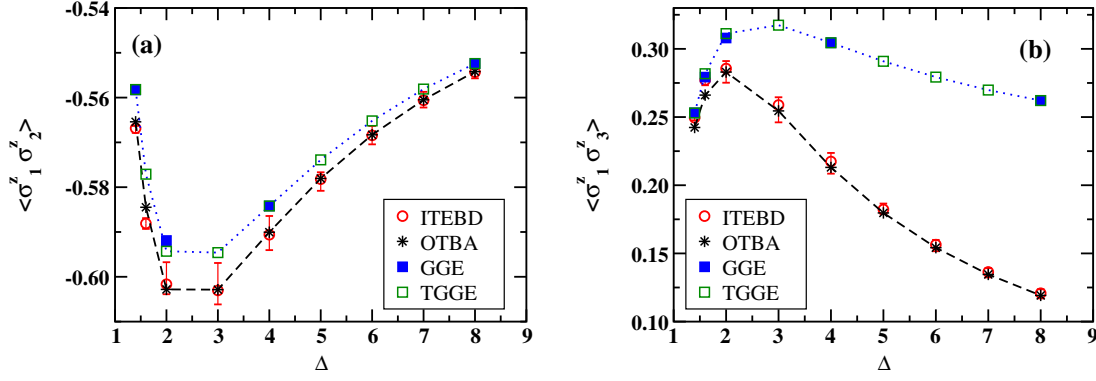
FIG. 2 (color online). Δ dependence of the ITEBD (red circles with error bars), overlap TBA (black stars), full GGE [37] (full blue squares), and truncated GGE (empty green squares) results for the large time expectation values (a) $\langle \sigma_1^z \sigma_2^z \rangle$ and (b) $\langle \sigma_1^z \sigma_3^z \rangle$ after the quench from the dimer initial state (4).

Overlap thermodynamic Bethe ansatz.—The OTBA method is formulated in the framework of the Bethe ansatz [60], used to diagonalize the *XXZ* Hamiltonian (2). Eigenfunctions corresponding to spin waves of M flipped spins on a chain of length L are parametrized by a set of M complex numbers $\{\lambda_j\}$, called rapidities. Spin waves can form bound states described by specific configurations of rapidities, called strings [61]. In the thermodynamic limit (TDL), defined by $M \to \infty$, $L \to \infty$ with M/L fixed, it is convenient to introduce the densities $\rho_n(\lambda)$ of n strings in rapidity space, together with the densities $\rho_n^h(\lambda)$ of unoccupied levels (holes).

The quench-action approach of Ref. [41] has been developed to describe the steady state following a quantum quench in Bethe ansatz integrable systems and has been implemented before for the transverse field Ising chain [41] and the Lieb-Liniger model [34]. This variational approach selects the relevant states by minimizing the generalized free energy (quench action)

$$S(\{\rho_n\}) = -\frac{2}{L} \mathrm{Re} \ln \langle \Psi_0 | \{\rho_n(\lambda)\} \rangle - s(\{\rho_n(\lambda)\}). \quad (5)$$

The first term involves the overlap between the initial state $|\Psi_0\rangle$ and the steady state $|\{\rho_n(\lambda)\}\rangle$, characterized by the string densities $\{\rho_n(\lambda)\}$. The exact overlaps were computed for the Néel state (3) in Refs. [62–65]. Here, we also generalized the overlap formula for the dimer product state (4) along the lines of Ref. [63]. In the TDL, the logarithm of both overlaps can be written as

$$-\frac{2}{L} \mathrm{Re} \ln \langle \Psi_0 | \{\rho_n(\lambda)\} \rangle = \sum_{n=1}^{\infty} \int_{-\pi/2}^{\pi/2} d\lambda \, \rho_n(\lambda) g_n(\lambda) \quad (6)$$

with the $g_n(\lambda)$ functions given by

$$g_1^N(\lambda) = -\ln \frac{\tan(\lambda + \frac{i\eta}{2}) \tan(\lambda - \frac{i\eta}{2})}{4\sin^2(2\lambda)}, \quad (7a)$$

$$g_1^D(\lambda) = -\ln \frac{\sinh^4(\eta/2) \cot^2(\lambda)}{\sin(2\lambda + i\eta) \sin(2\lambda - i\eta)} \quad (7b)$$

for the Néel and dimer states, respectively. In both cases, $g_n^{N,D}(\lambda) = \sum_{j=1}^{n} g_1^{N,D}[\lambda + (i\eta/2)(n+1-2j)]$ for higher strings ($n > 1$).

The second term $s(\{\rho_n(\lambda)\})$ in Eq. (5) is the entropy density [61,66] accounting for the number of microstates realizing the set of macroscopic $\{\rho_n(\lambda)\}$

$$s(\rho_n) = \sum_{n=1}^{\infty} \int d\lambda \frac{1}{2} \left[\rho_n \ln \frac{\rho_n + \rho_n^h}{\rho_n} + \rho_n^h \ln \frac{\rho_n + \rho_n^h}{\rho_n^h} \right]. \quad (8)$$

It is exactly half of the standard Yang-Yang entropy density [61,66] due to the fact that only parity invariant microstates have nonzero overlap [34,65].

The quench action (5) expresses the idea that the states relevant in the TDL are those with both large overlaps with the initial state and a large number of microscopic realizations. The steady state is captured by a saddle-point set of string densities, with the saddle-point approximation becoming exact in the TDL. The densities $\{\rho_n(\lambda)\}$ and $\{\rho_n^h(\lambda)\}$ are, however, not independent; interactions couple the rapidities of all the spin excitations, as expressed by the Bethe equations. As a consequence, the densities $\{\rho_n\}$ and $\{\rho_n^h\}$ satisfy coupled integral equations (constraints) [61]

$$a_n(\lambda) = \rho_n(\lambda) + \rho_n^h(\lambda) + \sum_{m=1}^{\infty} [T_{nm} \circ \rho_m](\lambda). \quad (9)$$

Here, $[a \circ b](\lambda) = \int_{-\pi/2}^{\pi/2} d\lambda' a(\lambda - \lambda') b(\lambda')$ denotes convolution, and the interaction kernel is expressed as $T_{nm} = (1 - \delta_{n,m}) a_{|n-m|} + a_{n+m} + 2 \sum_{j=1}^{\min\{n,m\}-1} a_{|n-m|+2j}$, with $\pi a_n(\lambda) = \sinh(n\eta)/[\cosh(n\eta) - \cos(2\lambda)]$ and $\cosh \eta = \Delta$. The constrained extremum of $S(\{\rho_n(\lambda)\})$ is then found through the standard treatment [61] and leads to the following integral equations for the functions $\eta_n(\lambda) \equiv \rho_n^h(\lambda)/\rho_n(\lambda)$:

$$\ln \eta_n(\lambda) = g_n(\lambda) + \mu n + \sum_{m=1}^{\infty}[T_{nm}\circ \ln(1+\eta_m^{-1})](\lambda). \quad (10)$$

Here, μ is a Lagrange multiplier introduced to fix the overall magnetization to zero. By examining $g_n(\lambda)$, we obtained for both initial states that $\ln \eta_n \sim \eta n^2$ for large n. This implies that the higher strings are suppressed as $\propto e^{-\eta n^2}$, so the infinite set of equations (10) can be safely truncated to relatively few equations and solved numerically. Having the numerical solution for η_n at hand, we can replace them into Eq. (9) and determine the densities efficiently. (For further technical details see Ref. [59]).

OTBA consistency checks.—There are several ways to check that the numerically obtained saddle-point string densities $\{\rho_n^*\}$ are, indeed, correct and correspond to the right initial states and to the right saddle point. A nontrivial check is provided by the computation of the norm of the initial state in the TDL, i.e.,

$$0 = -\frac{1}{L}\ln\langle\Psi_0|\Psi_0\rangle = \mathcal{S}(\{\rho_n^*(\lambda)\}), \quad (11)$$

with the quench action Eq. (5) evaluated via Eqs. (8) and (6) for the saddle-point solution. Equation (11) is, indeed, satisfied by our saddle-point solution within the accuracy of our numerical simulations $O(10^{-8})$. Notice that if this integral sum rule was violated, then the spectral weight of the saddle-point solution would be zero in the TDL.

Another important consistency check is provided by the expectation values of the conserved charges. These can be expressed in terms of the saddle-point densities as [67]

$$\langle\hat{Q}_{2m}\rangle = \sum_{n=1}^{\infty}\int_{-\pi/2}^{\pi/2}d\lambda\rho_n^*(\lambda)q_n^{(2m)}(\lambda), \quad (12)$$

with $q_n^{(2m)}(\lambda) = 2\pi\sum_{j=1}^{n}[-(\partial/\partial\lambda)]^{2m}a_1[\lambda + (i\eta/2)(n+1-2j)]$ the energy, in particular, being given by $E = 2\sinh\eta\langle\hat{Q}_2\rangle$. The saddle-point values of these charges must equal their values in the initial states. These latter were computed for the symmetric Néel state in Refs. [35,36]. Here, we determined them using both these methods in the symmetrized dimer state $|\Psi_0^D\rangle$. We evaluated the first six nonzero charges $\{\langle\hat{Q}_{2m}\rangle\}_{m=1,\dots,6}$ and compared them with the expectation values computed from Eq. (12). Excellent agreement up to more than 8 digits is found in all cases, providing a further stringent verification of the OTBA solution.

Steady-state correlations.—With the saddle-point string densities at hand, we then computed various short distance correlation functions in the steady state by making use of the recent results of two of the present authors, who provided exact formulas for the 2-point correlation functions in terms of the string densities [68]. We compared these values with the results of our ITEBD simulations.

Excellent agreement is found between OTBA and ITEBD for both initial states and for all $\Delta > 1$ values (cf. Figs. 1 and 2 and the Supplemental Material [58] for detailed numerical data). This establishes the quench-action-approach-based OTBA as a correct description of the steady state and the failure of GGE at the same time.

Discussion.—In this Letter, we studied various correlation functions in the asymptotic steady states for quantum quenches in the *XXZ* spin chain. We found that the predictions of the generalized Gibbs ensemble differ significantly from the results of real-time ITEBD simulations in the dimer case, thereby signaling the breakdown of the GGE. We also determined these asymptotic correlators by applying the quench-action-based overlap TBA description of the steady state and obtained numerically accurate predictions. We found that while the quench-action-based OTBA correctly captures the asymptotic steady state, the GGE fails for the states considered here. Finding a macroscopic statistical ensemble description of the steady state and clarifying the conditions for the validity of the GGE in strongly interacting systems, therefore, remain intriguing open questions.

Note added.—During the final stages of this work, a related paper appeared [43] that independently arrived at Eq. (7a) and in which the difference between the GGE and the OTBA predictions for nearest-neighbor correlators in the quench starting from the Néel state was observed as well.

*Corresponding author.
takacsg@eik.bme.hu

[1] T. Kinoshita, T. Wenger, and D. S. Weiss, Nature (London) **440**, 900 (2006).

[2] M. Cheneau, P. Barmettler, D. Poletti, M. Endres, P. Schauss, T. Fukuhara, C. Gross, I. Bloch, C. Kollath, and S. Kuhr, Nature (London) **481**, 484 (2012).

[3] S. Trotzky, Y.-A. Chen, A. Flesch, I. P. McCulloch, U. Schollwöck, J. Eisert, and I. Bloch, Nat. Phys. **8**, 325 (2012).

[4] T. Fukuhara, P. Schauß, M. Endres, S. Hild, M. Cheneau, I. Bloch, and C. Gross, Nature (London) **502**, 76 (2013).

[5] A. Polkovnikov, K. Sengupta, A. Silva, and M. Vengalattore, Rev. Mod. Phys. **83**, 863 (2011).

[6] C. Kollath, A. M. Läuchli, and E. Altman, Phys. Rev. Lett. **98**, 180601 (2007).

[7] M. Rigol, V. Dunjko, and M. Olshanii, Nature (London) **452**, 854 (2008).

[8] T. Barthel and U. Schollwöck, Phys. Rev. Lett. **100**, 100601 (2008).

[9] M. Rigol, Phys. Rev. Lett. **103**, 100403 (2009).

[10] M. Cramer and J. Eisert, New J. Phys. **12**, 055020 (2010).

[11] L. F. Santos and M. Rigol, Phys. Rev. E **81**, 036206 (2010).

[12] P. Barmettler, M. Punk, V. Gritsev, E. Demler, and E. Altman, New J. Phys. **12**, 055017 (2010).

[13] M. C. Bañuls, J. I. Cirac, and M. B. Hastings, Phys. Rev. Lett. **106**, 050405 (2011).

[14] P. Calabrese, F. H. L. Essler, and M. Fagotti, Phys. Rev. Lett. **106**, 227203 (2011).

[15] P. Calabrese, F. H. L. Essler, and M. Fagotti, J. Stat. Mech. (2012) P07016.

[16] N. Sedlmayr, J. Ren, F. Gebhard, and J. Sirker, Phys. Rev. Lett. **110**, 100406 (2013).

[17] M. Marcuzzi, J. Marino, A. Gambassi, and A. Silva, Phys. Rev. Lett. **111**, 197203 (2013).

[18] D. Iyer, H. Guan, and N. Andrei, Phys. Rev. A **87**, 053628 (2013).

[19] M. Rigol, V. Dunjko, V. Yurovsky, and M. Olshanii, Phys. Rev. Lett. **98**, 050405 (2007).

[20] M. A. Cazalilla, Phys. Rev. Lett. **97**, 156403 (2006).

[21] D. Rossini, A. Silva, G. Mussardo, and G. E. Santoro, Phys. Rev. Lett. **102**, 127204 (2009).

[22] P. Calabrese, F. H. L. Essler, and M. Fagotti, J. Stat. Mech. (2012) P07022.

[23] M. A. Cazalilla, A. Iucci, and M.-C. Chung, Phys. Rev. E **85**, 011133 (2012).

[24] V. Gurarie, J. Stat. Mech. (2013) P02014.

[25] M. Fagotti and F. H. L. Essler, Phys. Rev. B **87**, 245107 (2013).

[26] M. Collura, S. Sotiriadis, and P. Calabrese, Phys. Rev. Lett. **110**, 245301 (2013).

[27] M. Fagotti, J. Stat. Mech. (2014) P03016.

[28] M. Kormos, M. Collura, and P. Calabrese, Phys. Rev. A **89**, 013609 (2014).

[29] S. Sotiriadis and P. Calabrese, J. Stat. Mech. (2014) P07024.

[30] A. C. Cassidy, C. W. Clark, and M. Rigol, Phys. Rev. Lett. **106**, 140405 (2011).

[31] T. M. Wright, M. Rigol, M. J. Davis, and K. V. Kheruntsyan, Phys. Rev. Lett. **113**, 050601 (2014).

[32] J.-S. Caux and R. M. Konik, Phys. Rev. Lett. **109**, 175301 (2012).

[33] M. Kormos, A. Shashi, Y.-Z. Chou, J.-S. Caux, and A. Imambekov, Phys. Rev. B **88**, 205131 (2013).

[34] J. De Nardis, B. Wouters, M. Brockmann, and J.-S. Caux, Phys. Rev. A **89**, 033601 (2014).

[35] B. Pozsgay, J. Stat. Mech. (2013) P07003.

[36] M. Fagotti and F. H. L. Essler, J. Stat. Mech. (2013) P07012.

[37] M. Fagotti, M. Collura, F. H. L. Essler, and P. Calabrese, Phys. Rev. B **89**, 125101 (2014).

[38] D. Fioretto and G. Mussardo, New J. Phys. **12**, 055015 (2010).

[39] G. Mussardo, Phys. Rev. Lett. **111**, 100401 (2013).

[40] S. Sotiriadis, G. Takács, and G. Mussardo, Phys. Lett. B **734**, 52 (2014).

[41] J.-S. Caux and F. H. L. Essler, Phys. Rev. Lett. **110**, 257203 (2013).

[42] J.-S. Caux, in Proceedings of the Workshop on Emergent Phenomena in the Dynamics of Quantum Matter, New York, 2014 (unpublished).

[43] B. Wouters, M. Brockmann, J. De Nardis, D. Fioretto, M. Rigol, and J.-S. Caux, preceding Letter, Phys. Rev. Lett. **113**, 117202 (2014)].

[44] A. Auerbach, Interacting Electrons and Quantum Magnetism (Springer, New York, 1994).

[45] F. H. L. Essler and R. M. Konik, in From Fields to Strings: Circumnavigating Theoretical Physics, edited by Misha Shifman, Arkady Vainshtein, and John Wheater, Ian Kogan Memorial Collection Vol. 3 (World Scientific, Singapore, 2004), p. 684.

[46] P. Calabrese and J. Cardy, J. Stat. Mech. (2005) P04010.

[47] P. Calabrese and J. Cardy, Phys. Rev. Lett. **96**, 136801 (2006).

[48] A. B. Kuklov and B. V. Svistunov, Phys. Rev. Lett. **90**, 100401 (2003).

[49] L.-M. Duan, E. Demler, and M. D. Lukin, Phys. Rev. Lett. **91**, 090402 (2003).

[50] T. Barthel, C. Kasztelan, I. P. McCulloch, and U. Schollwöck, Phys. Rev. A **79**, 053627 (2009).

[51] J. Simon, W. S. Bakr, R. Ma, M. E. Tai, P. M. Preiss, and M. Greiner, Nature (London) **472**, 307 (2011).

[52] Y.-A. Chen, S. Nascimbène, M. Aidelsburger, M. Atala, S. Trotzky, and I. Bloch, Phys. Rev. Lett. **107**, 210405 (2011).

[53] C. K. Majumdar and D. K. Ghosh, J. Math. Phys. (N.Y.) **10**, 1388 (1969).

[54] G. Vidal, Phys. Rev. Lett. **93**, 040502 (2004).

[55] G. Vidal, Phys. Rev. Lett. **98**, 070201 (2007).

[56] This approach is justified in the TDL, where off-diagonal contributions vanish.

[57] The region of validity of the ITEBD simulations was determined by comparing results using different bond dimensions and the observed saturation of the entanglement. Our real-time simulation results are consistent with those obtained in Ref. [37].

[58] See the Supplemental Material at http://link.aps.org/supplemental/10.1103/PhysRevLett.113.117203 for details of the ITEBD simulation and numerical data.

[59] B. Pozsgay, M. Mestyán, M. A. Werner, M. Kormos, and G. Takács (to be published).

[60] H. Bethe, Z. Phys. **71**, 205 (1931).

[61] M. Takahashi, Thermodynamics of One-Dimensional Solvable Models (Cambridge University Press, Cambridge, England, 1999).

[62] K. K. Kozlowski and B. Pozsgay, J. Stat. Mech. (2012) P05021.

[63] B. Pozsgay, J. Stat. Mech. (2014) P06011.

[64] M. Brockmann, J. De Nardis, B. Wouters, and J.-S. Caux, J. Phys. A **47**, 145003 (2014).

[65] M. Brockmann, J. De Nardis, B. Wouters, and J.-S. Caux, arXiv:1403.7469.

[66] C. N. Yang and C. P. Yang, J. Math. Phys. (N.Y.) **10**, 1115 (1969).

[67] M. Lüscher, Nucl. Phys. **B117**, 475 (1976).

[68] M. Mestyán and B. Pozsgay, arXiv:1405.0232 [J. Stat. Mech. (to be published)].